

MULTIPLE PRODUCTION OF PARTICLES IN COLLISIONS BETWEEN 9 GEV PROTONS AND NUCLEONS

V. S. BARASHENKOV, V. A. BELYAKOV, E. G. BUBELEV, WANG SHOU FENG,
V. M. MALTSEV, TEN GYN and K. D. TOLSTOV

*Joint Institute of Nuclear Research, Laboratory of Theoretical Physics and High Energy Laboratory,
Dubna, USSR*

Received 25 June 1958

Abstract: Some theoretical calculations pertaining to multiple production of particles in nucleon-nucleon collisions at 7–10 GeV were presented in ref.¹). Some preliminary experimental results obtained by irradiating photographic emulsions with the proton beam from the synchrocyclotron of the Joint Institute of Nuclear Research were given in ref.²). In the present paper we compare the theoretical results of ref.¹) with the results of some new experiments. 372 stars, of which 50 were classified as proton-nucleon collisions, were recorded in NIKFI-R photographic emulsions along the tracks of ≈ 9 GeV protons accelerated in the JINR proton synchrocyclotron. The mean number of charged particles created in these collisions was 3.6 ± 0.5 . The angular distribution of fast charged particles is obtained. As a whole the experimental results agree with the statistical theory of multiple particle production within the limits of the experimental errors. Some discrepancy is evident in the small angle range and may be due to the contribution of non-central impacts and to asymmetry of the angular distribution in the c.m.s.

1. Selection of Nucleon Interactions

With the help of a plunger-type target the $\approx 450 \mu$ thick NIKFI-R photographic emulsions were introduced into the vacuum chamber of the accelerator and irradiated with protons of an energy of ≈ 9 GeV in the JINR proton synchrocyclotron.

After treatment the emulsions were examined under a magnification of 945 along the tracks of the primary protons. In this way all interaction events including scattering through angles $> 3^\circ$ could be reliably recorded. The tracks of δ electrons produced by 9 GeV protons resembled straight relativistic tracks and hence in order to remove these impurities from the results, observations were carried out along such tracks. In three sets of measurements in which 372 stars were recorded (108 in single emulsions and 100 and 164 in emulsion stacks) 39 stars were found (9, 10 and 20 respectively in the three series) which possessed an even number of rays, no recoil nucleus or β -electron track and finally possessed not more than one grey or black track, the black tracks being observed only in the front hemisphere. Stars of this type were ascribed to interactions between the accelerated protons and free

or quasi-free protons of the emulsion nuclei, that is, to (pp) collisions.

The number of (pp) collisions is larger than one would expect from the total number of stars if the amount of hydrogen atoms in the emulsion is taken into account; however, it should be kept in mind that in a number of experiments at smaller energies approximately equal numbers of free and quasi free (pp) collisions were obtained.

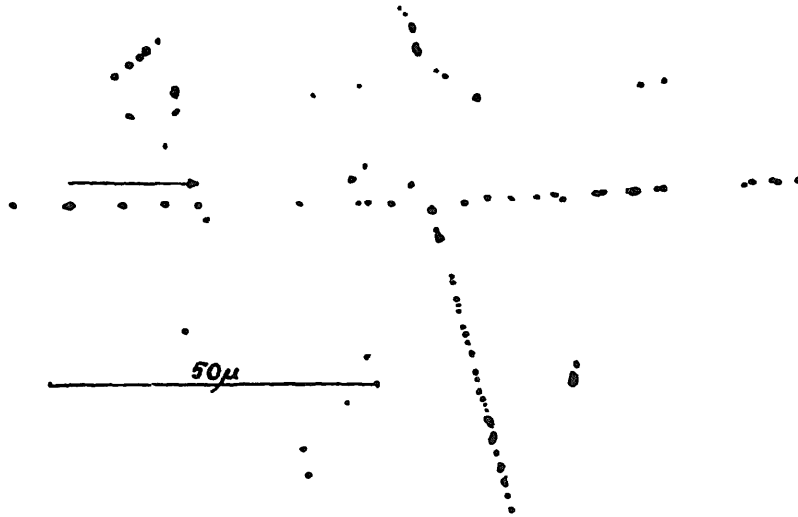


Fig. 1. Example of a star classified as an elastic (pp) collision event.

Three co-planar events satisfying the corresponding kinematic requirements were classified as elastic scattering. The photograph in fig. 1 is an example of an elastic (pp) collision selected in this way.

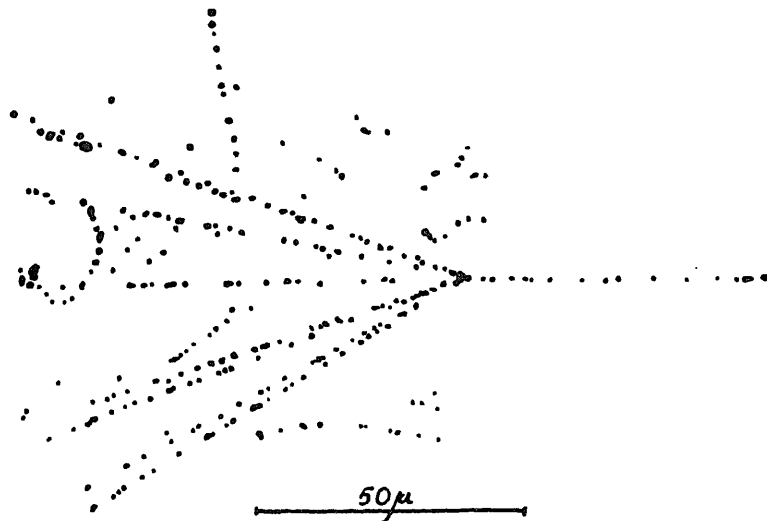


Fig. 2. (pp) collision involving the creation of 8 charged relativistic particles.

36 events were ascribed to inelastic (pp) collisions. An example of an inelastic (pp) collision chosen in this manner is shown in the photograph in fig. 2.

In an emulsion stack containing 264 stars 11 events were classified as proton-neutron, (pn), collisions. These stars had an odd number of prongs and do not exhibit recoil nuclei.

An example of a collision of this type is shown in fig. 3.

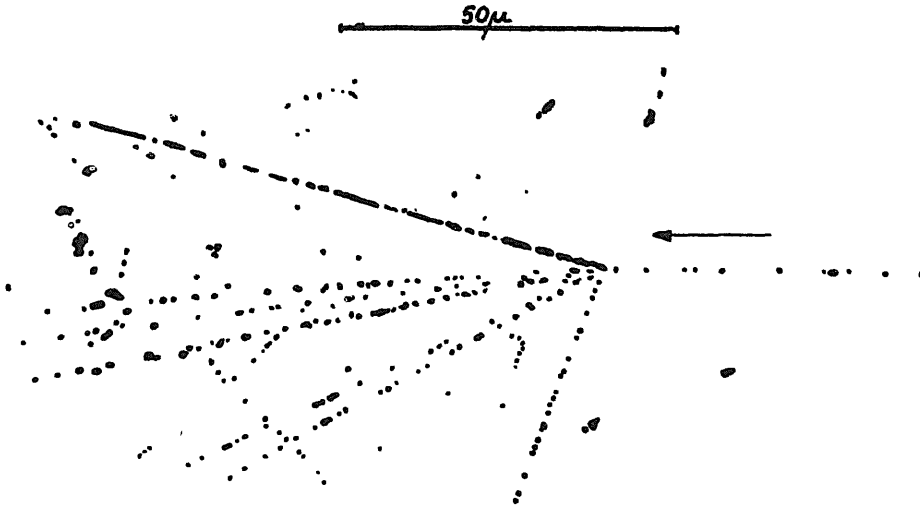


Fig. 3. (pn) collision involving the creation of 5 charged relativistic particles.

2. Prong Distribution of Stars

The prong distribution of stars referring to 37 inelastic (pp) collisions is shown in table 1. (After introduction of a geometric correction a 2-prong case was added). The average number of charged particles in (pp) collisions is

TABLE 1

Number of stars	13	17	5	2
Number of prongs	2	4	6	8

$\bar{n}_p = 3.8 \mp 0.3$. The experimental values satisfactorily agree with the value $\bar{n}_p \approx 3.5$ for (pp) collisions calculated on basis of the statistical theory of multiple production by employing the tabulated values in ref.¹⁾ for 10 GeV protons. If generation of strange particles is taken into account the theoretical values should be larger by a few percent.

Since the number of (pn) collisions was small, their prong distribution will not be given in this article. The average number of charged particles created

in (pn) collisions was $\bar{n}_n = 2.8 \pm 0.6$, which satisfactorily agrees with the theoretical value $\bar{n}_n \approx 3.2$ ¹⁾.

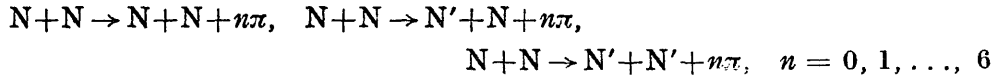
In stars due to proton-nucleon collisions "fast particles" $n^{(s)}$ were singled out whose ionization losses $I \leq 1.4I_0$, where I_0 are ionization losses corresponding to the relativistic ionization plateau. Protons with an energy $E_p \geq 0.5$ GeV as well as π mesons with $E_\pi \geq 0.08$ GeV are considered to be $n^{(s)}$ particles. The particle frequency distribution for 37 inelastic (pp) collisions is presented in table 2. The average number of $n^{(s)}$ per star is

TABLE 2

Number of stars	9	6	7	8	2	3	1	1
Number of particles	1	2	3	4	5	6	7	8

$\bar{n}_{(pp)}^{(s)} = 3.2 \pm 0.3$. In a similar manner "fast particles" were selected from (pn) collisions. The average number of "fast particles" was $\bar{n}_{(pn)}^{(s)} = 2.5 \pm 0.6$.

In order to compare these data with the statistical theory of multiple creation we made use of the statistical weights given in ref.¹⁾ and under the same assumptions as employed there we calculated the momentum distributions of pions and nucleons created in the partial reactions



at $E = 10$ GeV¹⁾. (N' is the "isobar" symbol; see ref.¹⁾.)

The momentum distribution of pions and nucleons in the c.m.s. † integrated over the angles and averaged over all partial reactions is shown in fig. 4. The corresponding momentum distribution of pions and nucleons in the laboratory coordinate system is given in fig. 5. All momentum distributions are normalized to unity. (In our calculations we did not consider the small contribution of pions and nucleons created in reactions involving strange particles (see ref.¹⁾.) From the spectra presented above it follows that the contribution of "slow" pions ($E_\pi < 0.08$ GeV) and "slow" nucleons ($E_n < 0.5$ GeV) is small ($\approx 10\%$). Therefore the average numbers of "fast" charged particles $\bar{n}_p^{(s)}$ and $\bar{n}_n^{(s)}$ computed theoretically are only a few per cent smaller than the average theoretical numbers of charged particles \bar{n}_p and \bar{n}_n : $\bar{n}_p^{(s)} \approx 3.1$, $\bar{n}_n^{(s)} \approx 2.9$. Experimentally it has been found that the fraction of "slow" particles is $15\% \pm 5\%$ of the total number of charged particles, about $\frac{2}{3}$ of them being protons. The mean energy of these protons was (120 ± 40) MeV.

† In the calculations, use was made of the nomograms made by L. G. Zastavenko (to be published).

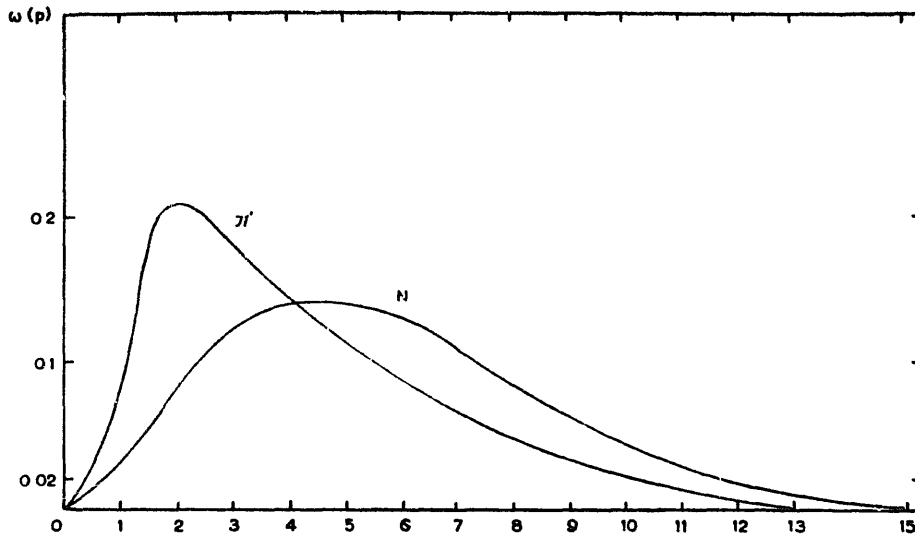


Fig. 4. Momentum distributions of pions and nucleons produced in (NN) collisions. C.m.s. Momentum values in $m_\pi c$ units are plotted along the abscissa axis.

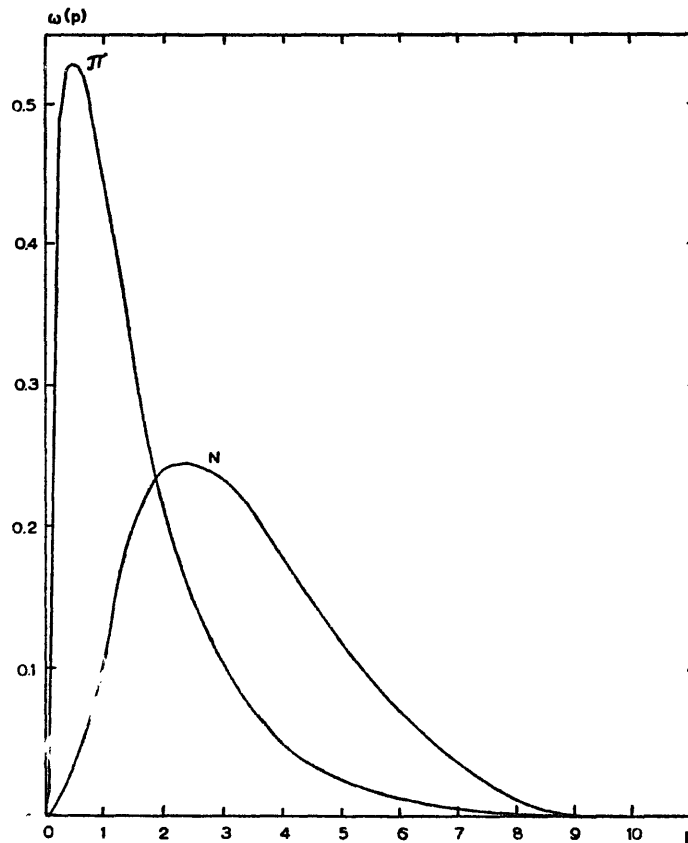


Fig. 5. Momentum distributions of pions and nucleons produced in (NN) collisions. Laboratory system. Momentum values in GeV/c units plotted along the abscissa axis.

There is good agreement between the theoretical and experimental values, $\bar{n}_p^{(s)}$ and $\bar{n}_n^{(s)}$ †. However, one notes that the fraction of “slow” protons is comparatively high.

3. Angular Distribution of Prongs in (pp) Stars

The histogram in fig. 6 represents the experimental angular distribution of particles $n_p^{(s)}$ emitted in a solid angle $\Delta\Omega = \Omega(\theta_2) - \Omega(\theta_1)$ in the laboratory system. The angle which contains half of particles $n_p^{(s)}$ is $\varphi_{\frac{1}{2}} = 16^\circ$. The

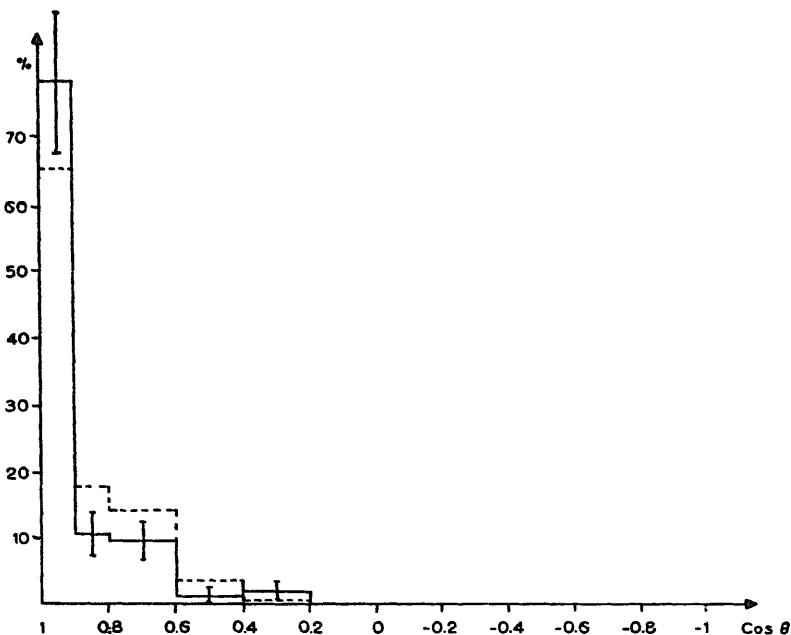


Fig. 6. Angular distribution of fast charged particles emitted in (pp) collisions in a solid angle $\Delta\Omega = \Omega(\theta_2) - \Omega(\theta_1)$. The continuous histogram is the experimental values. The dotted curve is the theoretical histogram. The values of angle θ are plotted along the abscissa axis. Laboratory system of coordinates.

angular distribution of pions and nucleons in the laboratory system was computed by the aid of the momentum distribution in fig. 4. under the assumption of an isotropic distribution in the c.m.s. This distribution is represented in fig. 7. The angular distributions of pions $W_\pi(\theta)$ and nucleons $W_N(\theta)$ are normalized, so that $\int_0^\pi W(\theta) \sin \theta d\theta = 1$. The angular distributions for “fast” particles $n^{(s)}$ only slightly differ from the total angular distributions. From Fig. 7 it can be seen that the nucleon angular distribution has a larger for-

† In reactions involving more than one pion ($n_\pi > 1$), the average number of charged pions is near to $\frac{2}{3}$ of the total number ($\bar{n}_p^{(t)} = 3.4$; $\bar{n}_n^{(t)} = 3.3$) and the number of protons on the average is close to 1.2 for (pp) collisions and to unity for (pn) collisions (see ref.³).

ward asymmetry than pions and this corresponds to the fact that the nucleon spectrum $W_N(p)$ is harder than the pion spectrum $W_\pi(p)$ (see figs. 4 and 5). The average number of "fast" charged particles $n^{(g)}$ emerging in the solid angle was computed with the help of the angular distribution in fig. 7. The

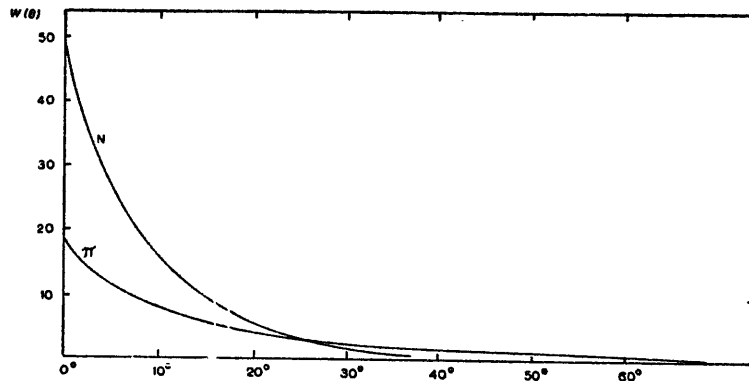


Fig. 7. Angular distribution of pions and nucleons produced in (NN) collisions. Emission angle θ plotted along abscissa axis. Laboratory system.

results of these calculations are presented in fig. 6. Within the experimental errors they satisfactorily agree with the experiments. However, in the small angle region there is an appreciable discrepancy as is evident from table 3.

TABLE 3

Angle range	Number of particles		
	Calculated	Experimental	Exp./calc.
0-3	4	9	2.2
0-5	10	19	1.9
0-10	28	39	1.4

This difference may possibly be due to an admixture of particles created by a process which cannot be described by statistical theorem I, e.g., by "peripheral collisions". A non-isotropic angular distribution corresponds to this in the c.m.s. †. It is likewise possible that the large fraction of observed "slow" protons (see above) is also related to this circumstance. These conclusions are close to those arrived at by analysis of cosmic ray experiments⁵⁾. However, a final conclusion would require a larger amount of statistical material and a more rigorous analysis.

We now estimate the mean energy losses during pion production in (pp)

† I. I. Gurevich⁴⁾ who investigated emulsions irradiated by cosmic rays also arrived at the conclusion that at an energy $\approx 10^{10}$ eV there is some asymmetry in the angular distribution in the c.m.s.

collisions. Taking into account the average number of charged and neutral pions created in a single (pp) collision, $\bar{n}_\pi = 3.7 \pm 0.5$, we find that for the pion momentum distribution shown in fig. 5, the mean energy expended by a primary nucleon in pion production is $\Delta E \approx 50\%$ of its initial energy.

In conclusion the authors are glad to thank D. I. Blokhintsev for numerous discussions of various aspects of the theory of multiple particle production and also the proton synchrocyclotron crew of the High Energy Laboratory for making these experiments possible.

Appendix

In reducing experimental results and preparing experiments it is quite frequently necessary to know the momentum distribution of pions produced in (NN) collisions for a given emission angle θ in the laboratory system.

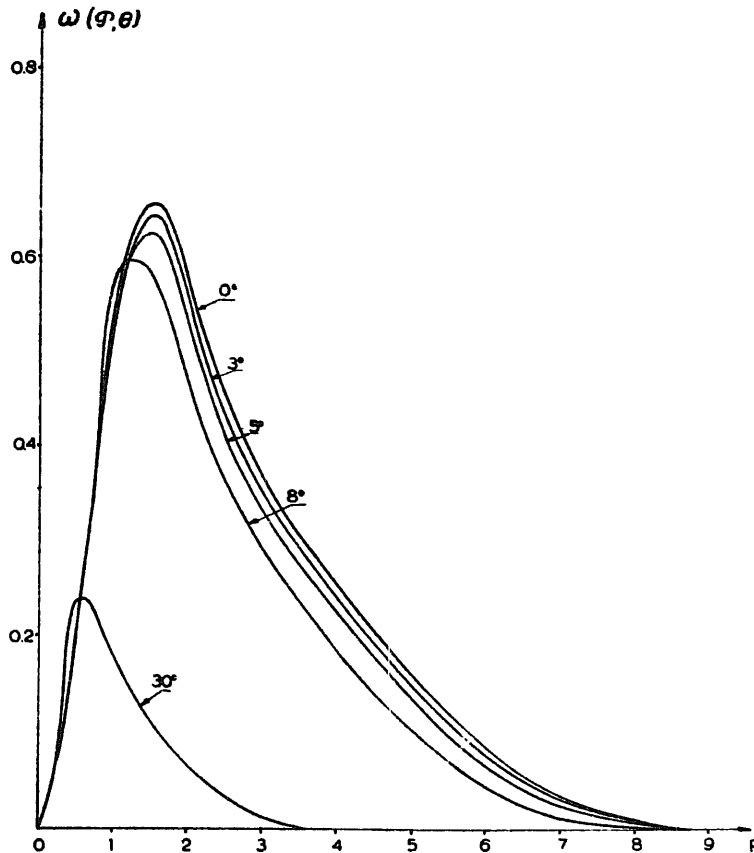


Fig. 8. Momentum spectrum of pions produced in (NN) collisions at angles of $\theta = 0^\circ, 3^\circ, 5^\circ, 8^\circ, 30^\circ$ in the laboratory system. Momentum in GeV/c units plotted along abscissa axis.

Distributions of this type computed in accord with ref.¹⁾ for angles $\theta = 0^\circ$, 3° , 5° , 8° , 30° are represented in fig. 8. Together with the angular distributions in fig. 7 these distributions were used by us for calculation of the data in table 3.

References

- 1) V. S. Barashenkov *et al.*, Nuovo Cimento Supplement **7** (1958) 117
- 2) N. P. Bogachev *et al.*, Atomnaya Energyia **4** (1958) 281
- 3) S. Z. Belenky *et al.*, Uspekhi Fisich. Nauk **62** (1957 no. 2
- 4) I. I. Gurevich, Reports at Jubilee Conference of Moscow Engineering-Technical Institute (April 1958)
- 5) G. T. Zatsepin, Report at Seminar of High Energy Laboratory of Joint Institute of Nuclear Research (1958)